Journal of Catalysis **210,** 183–191 (2002)
doi:10.1006/jcat.2002.3672

The Effects of *in Situ* Fluorination and Support on the Hydrodenitrogenation of Methylcyclohexylamine

Lianglong Qu and Roel Prins[1]

Laboratory for Technical Chemistry, Federal Institute of Technology, ETH–Hönggerberg, 8093 Zurich, Switzerland

Received February 7, 2002; revised May 1, 2002; accepted May 1, 2002

The effects of *in situ* fluorination on the hydrodenitrogenation of methylcyclohexylamine have been studied at 310–350°C and 5.0 MPa in a continuous microflow reactor over sulfided and fluorinated sulfided NiMo catalysts supported on alumina and silica–alumina. The silica–alumina-supported catalysts exhibit higher hydrodenitrogenation activity than their alumina-supported counterparts. *In situ* fluorination promotes hydrodenitrogenation activity mainly by enhancing the elimination of NH_3 from methylcyclohexylamine, while less of an effect is observed for the direct reaction of methylcyclohexylamine to methylcyclohexane. Kinetic parameters were obtained for the reaction network by fitting the experimental results with Langmuir–Hinshelwood equations. After fluorination, the reaction rate constants of all catalysts increase substantially for the elimination step, but only slightly for the direct reaction. The activation energies and the heat of adsorption are about the same over all catalysts. This indicates that the intrinsic activity of the active sites is not influenced by the *in situ* fluorination or by the support, and only the number of sites active for hydrodenitrogenation is increased by a change of the dispersion of the active phase.

Key Words: **HDN; hydrodenitrogenation; methylcyclohexylamine; NiMo catalysts; *in situ* fluorination; alumina; silica–alumina.**

INTRODUCTION

Removal of organic nitrogen-containing compounds from oil fractions is of paramount importance in modern refining industries, especially when heavier feedstocks, coal-derived distillates, and oil shale, which contain more nitrogen compounds than conventional feedstocks, are processed (1). Conventionally fluorinated hydroprocessing catalysts are used in refineries in the hydrofining of lubricant oils (2–4). With increasing demand for hydrotreating, fluorine is widely studied as an additive in hydrotreating and hydrocracking catalysts containing Mo and W supported on alumina, silica–alumina, and zeolites. As many patents on the use of fluorine as a promoter in hydrotreating and hydrocracking demonstrate (5–20), even if ways of introducing fluorine are different, some refineries are using fluorinated catalysts for hydrotreating and hydrocracking, at least in some regions of the world. Several studies have furthered the understanding of the effect of fluorine in hydrotreating catalysts (21–35), but only a few have dealt with HDN (22, 23, 25–28). The enhancement of the HDN activity by fluorine addition has been assigned to higher acidity, better dispersion, and higher chemisorption capacity for hydrogen. In most cases, fluorination is performed by impregnating the support with a fluoride salt, like NH_4F (see, e.g., Refs. 21, 28). After NH_4F impregnation, drying, and calcination, molybdenum and nickel are introduced as usual by impregnation. After a subsequent calcination, the resulting materials are sulfided in a stream of H_2S in H_2. The disadvantage of this method is that the dispersion of the resulting MoS_2 and Ni sulfides may be different in the fluorine-containing and fluorine-free NiMo catalysts. Conclusions about the effects of fluorine are then difficult to make. *In situ* fluorination, after preparation of the NiMo catalysts in their sulfidic form, has been described in patents (see, e.g., Refs. 36, 37), but not in the open literature. Because in this method the metal sulfides are prepared before fluorination, the catalyst dispersion might not be influenced by the fluorination and this might allow one to draw firm conclusions about the effects of fluorine in HDN.

In previous work, we found that *in situ* fluorination has a positive effect on the isomerization and no effect on the hydrogenation of cyclohexene (38). In this work, the effect of *in situ* fluorination of the sulfide NiMo catalysts supported on Al_2O_3 and amorphous silica–alumina (ASA) supports was studied. By comparing the kinetic parameters of the different catalysts, the effects of fluorination and the support on the activity and reaction network can be discussed.

Ortho-toluidine is a nitrogen-containing model compound convenient for studying the kinetics of the hydrodenitrogenation (HDN) reaction (39–41). The HDN of toluidine takes place mainly via hydrogenation to methylcyclohexylamine (MCHA). MCHA then reacts to methylcyclohexene (MCHE) and methylcyclohexane (MCH). Only traces of MCHA are detected as primary reaction intermediates in the HDN of *ortho*-toluidine because its rate of formation is much slower than its rate of further

[1] To whom correspondence should be addressed. Fax: 41-1-632 11 62. E-mail: prins@tech.chem.ethz.ch.

0021-9517/02 $35.00

reaction. MCHA has a strong inhibition effect on the HDN of *ortho*-toluidine.

C(sp^3)–N bond scission in MCHA can take place in two ways. The direct elimination of NH_3 from MCHA occurs by the removal of a hydrogen atom at the β-C atom relative to the amino group, followed by olefin saturation (42, 43). The other is the direct cleavage of the C–N bond in MCHA, which leads to MCH (39, 43–45). This complicates the kinetic modeling of the HDN network of *ortho*-toluidine and makes it difficult to obtain reliable kinetic parameters. Therefore, it is necessary to study the HDN of MCHA first.

EXPERIMENTAL

The catalysts containing 4 wt% Ni and 13 wt% Mo were prepared by pore volume impregnation of the supports, γ-Al_2O_3 (Condea), and ASA containing 25 wt% Al_2O_3 (prepared by the sol–gel method), with aqueous solutions of ammonium molybdate tetrahydrate (Fluka) and nickel nitrate hexahydrate (Fluka), followed by drying at 120°C overnight and calcination at 500°C in air after each impregnation step. The NiMo/Al_2O_3 catalyst has a pore volume of 0.42 ml/g and a surface area of 155 m^2/g by BET nitrogen adsorption. The NiMo/ASA catalyst has a pore volume of 0.43 ml/g and a surface area of 265 m^2/g. The HDN of MCHA was carried out over 0.02–0.05 g *in situ* fluorinated sulfided NiMo/Al_2O_3 and NiMo/ASA catalysts diluted with 8 g SiC in a high-pressure microreactor. The catalyst was dried for 2 h at 400°C and then sulfided with a mixture of 10% H_2S in H_2 at 1.0 MPa. Sulfidation started from ambient temperature with a slow increase for 14 h to 370°C and maintained for 2 h.

In situ fluorination was performed after the sulfidation step. The pressure was first increased to reaction condition (5.0 MPa) with the sulfiding gas. When the temperature of the reactor had decreased to 200°C, a solution of 0.26 wt% *ortho*-fluorotoluene in octane was dosed to the reactor at a rate of 0.0016 ml/min with a syringe pump. The temperature was slowly raised to 370°C and kept for 48 h (total fluorination duration, 55 h). The sulfiding gas was flowing through the reactor throughout the fluorination process. The final fluorine content of the catalysts was about 1 wt%, as determined by X-ray fluorescence analysis.

After activation, the temperature was adjusted to 350°C, and the sulfiding gas was replaced by pure hydrogen. A solution of MCHA, cyclohexene (CHE), octane (solvent), *n*-heptane (internal standard), and dimethyldisulfide (to generate H_2S *in situ*) was fed to the reactor. Partial pressures at the reactor inlet were $P_{MCHA} = 2, 4, 14, 24$, and 36 kPa, $P_{CHE} = 4$ kPa, $P_{H_2S} = 17.5$ kPa, $P_{H_2} = 4.8$ MPa, and octane as the balance. CHE was added to the reactants in order to monitor the hydrogenation of olefin in the presence of MCHA. Preliminary experiments showed that CHE had no influence on the HDN of MCHA.

The reaction products were analyzed by online gas chromatography (Varian Star 3400CX equipped with a 30-m DB-5MS fused silica capillary column and a flame ionization detector). All the kinetic data were obtained by varying weight time and reactant initial partial pressure after stabilization for 20 h onstream. Weight time was defined as $\tau = m_C/n_{feed,total}$, where m_C denotes the catalyst weight and $n_{feed,total}$ the total molar flow fed to the reactor. The hydrogen flow rate was always changed in proportion to the liquid flow rate. No diffusion or transport limitations were detected under the conditions studied. This allowed us to model the reaction with a Langmuir–Hinshelwood mechanism assuming adsorption equilibrium for the HDN compounds. The program used for the nonlinear numeric fitting was SCIENTIST® version 2.0 by MicroMath Inc.

RESULTS AND DISCUSSION

HDN Reaction Scheme of MCHA

The HDN network of MCHA is shown in Fig. 1. Even though the HDN of amines is quite simple, there are still two reaction pathways: the elimination of NH_3 to MCHE, followed by hydrogenation to MCH (path 1), and the direct production of MCH (path 2). This direct reaction is generally considered to occur by exchange of the NH_2 group by an SH group, followed by fast hydrogenolysis of the resulting *ortho*-methylcyclohexylthiol to MCH and H_2S (39, 43–47). For simplicity, we call this reaction the direct reaction.

The product distribution versus weight time plot shows that MCHE and MCH are both formed at small weight time and thus are primary products. Nevertheless, MCHE reaches a maximum and the MCH curve bends upward at larger weight time, indicating that MCH is also a product of MCHE (Figs. 2a and 2b). A trace of the isomerization

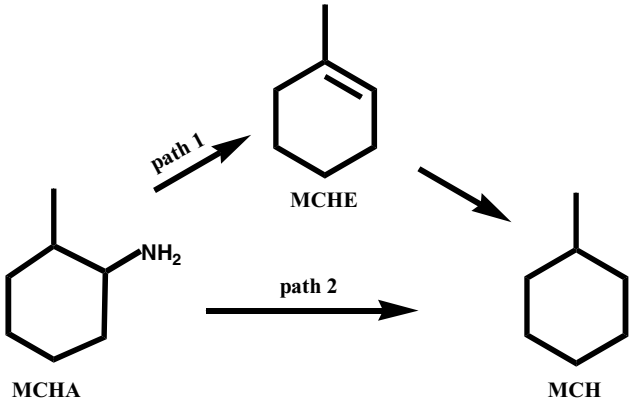

FIG. 1. Hydrodenitrogenation reaction network for methylcyclohexylamine (MCHA) over NiMo/Al_2O_3 and NiMo/ASA.

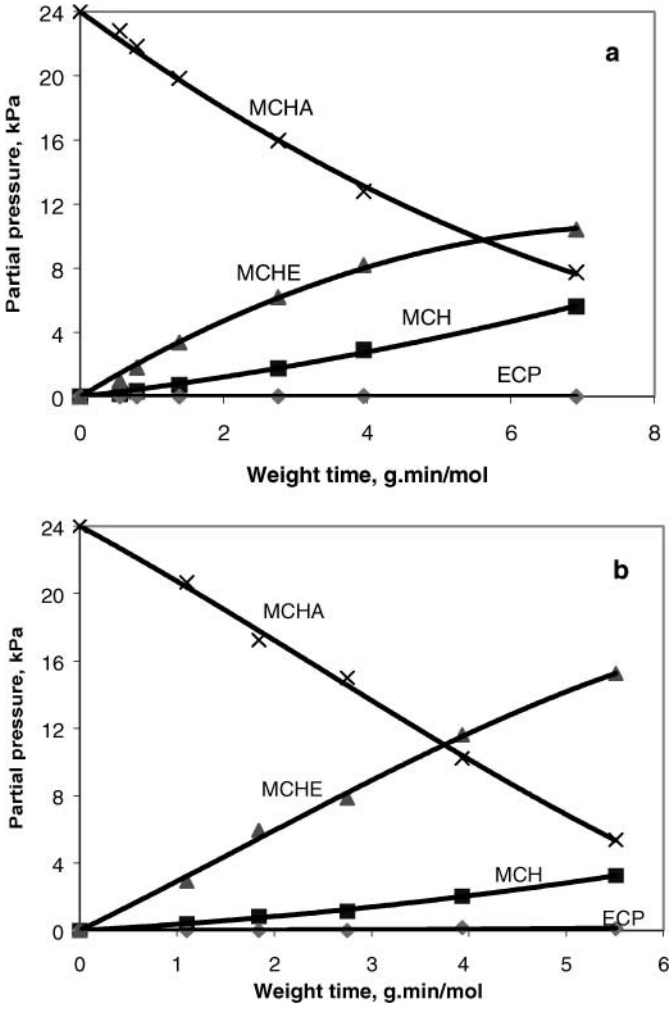

FIG. 2. Product distribution during the hydrodenitrogenation of 24 kPa methylcyclohexylamine (MCHA) at 350°C over (a) $NiMo/Al_2O_3$ and (b) NiMo/ASA catalysts.

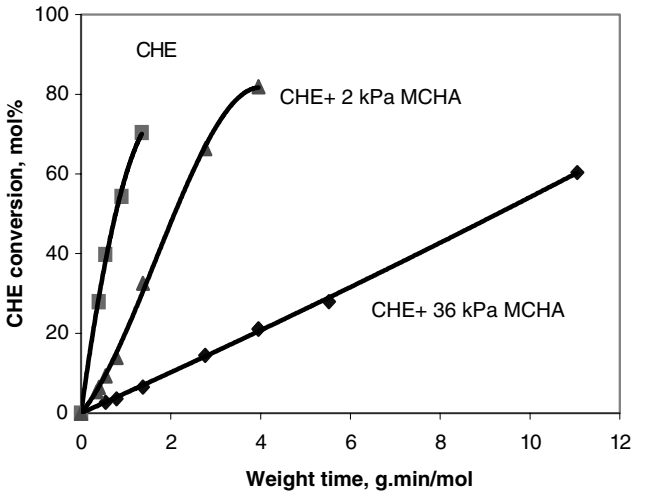

FIG. 3. Inhibition of methylcyclohexylamine (MCHA) on the hydrogenation of cyclohexene (CHE) at 350°C over $NiMo/Al_2O_3$.

product ethylcyclopentane (ECP) was formed at high temperature and longer weight time. The formation of ECP over NiMo/ASA and fluorinated catalysts was about as low as that over $NiMo/Al_2O_3$. MCHE is present in the product at a relatively high concentration until a very high MCHA conversion is reached. This indicates a strong inhibition of MCHA on the hydrogenation of MCHE by competitive adsorption, which is confirmed by a comparison of the results obtained with a mixed feed of MCHA and CHE and with a pure CHE feed (Fig. 3). With MCHA in the reaction mixture, isomerization of CHE to methylcyclopentane (MCP) did not take place.

Support Effect

The conversions of MCHA and CHE over the two catalyst systems show that the ASA-supported catalyst has a slightly higher HDN activity and lower olefin hydrogenation activity than its Al_2O_3-supported counterpart (Fig. 4). The latter conclusion is in agreement with our earlier findings on the effect of the support on the hydrogenation of pure CHE (38). Compared with Al_2O_3-supported catalysts, more MCHE is present in the products over ASA-supported catalysts, while the amount of MCH is almost the same (Fig. 5a). The same holds for the fluorinated catalysts (Fig. 5b). This means that the ASA support (with higher acidity) favors the elimination pathway of the HDN network. The direct reaction path either remains almost unchanged or the ASA-supported catalyst has a lower hydrogenation activity than the Al_2O_3-supported catalyst. We will come back to this point when discussing the kinetic

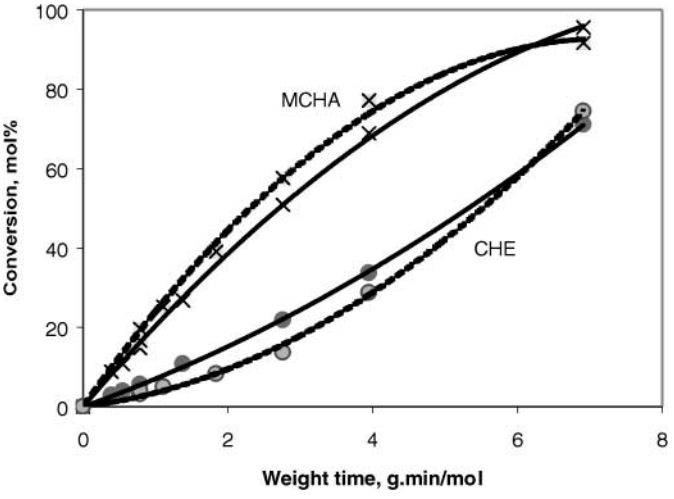

FIG. 4. Effect of the support on the hydrodenitrogenation of 14 kPa methylcyclohexylamine (MCHA) and the hydrogenation of 4 kPa cyclohexene (CHE) at 350°C over $NiMo/Al_2O_3$ (solid lines) and NiMo/ASA (dashed lines).

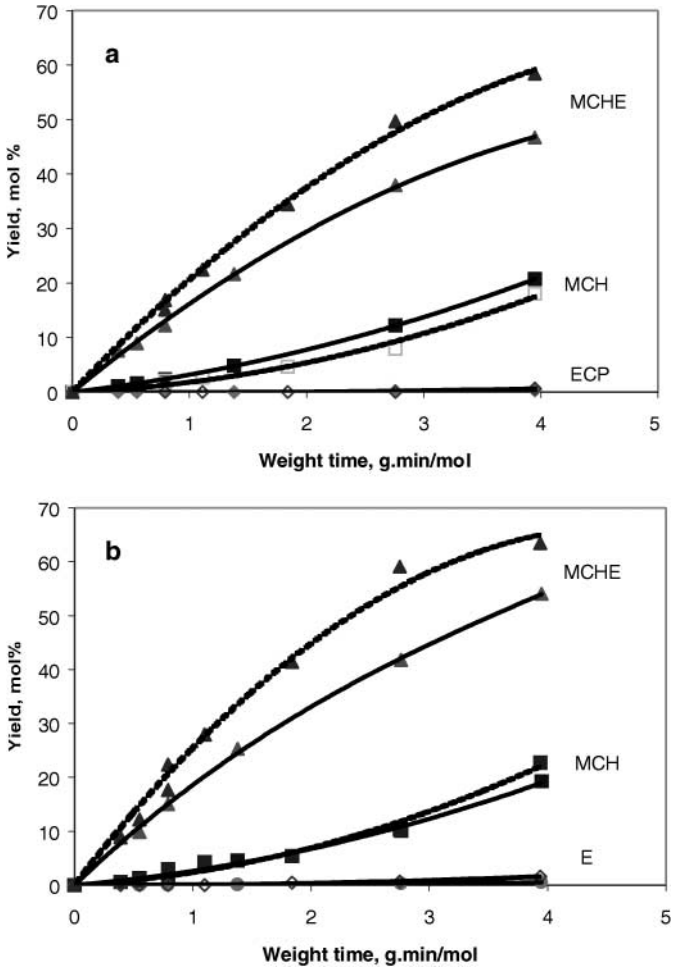

FIG. 5. Effect of the support on the yields of methylcyclohexene (MCHE) and methylcyclohexane (MCH) during the hydrodenitrogenation of 14 kPa methylcyclohexylamine at 350°C over (a) NiMo and (b) F–NiMo catalysts supported on Al_2O_3 (solid lines) and ASA (dashed line).

results. The MCHE formed by the elimination path is hydrogenated relatively slowly, owing to the strong inhibition of MCHA in the system. Thus, the MCHE yield reaches high values. The formation of ECP is substantial only when almost all the MCHA has been converted.

Minderhoud and van Veen (48) reported that an ASA-supported NiMo catalyst showed higher HDN, hydrocracking, and hydrodearomatization, but a lower hydrodesulfurization (HDS) activity than its Al_2O_3-supported counterpart. This indicates that the active centers for HDS and HDN are different. A similar detrimental effect of silica–alumina on the HDS activity was reported for CoMo and NiW catalysts (49–51). It was explained by the poorer dispersion of the molybdenum and tungsten phases on the silica–alumina support. Al_2O_3 and Al_2O_3-rich supports interact strongly with Mo and W oxide species due to the abundance of basic OH groups. SiO_2 and SiO_2-rich supports, on the other hand, promote agglomeration of Mo and W oxides because of a weak interaction (52). This is probably the case for our ASA support, which contains 75% SiO_2. However, an enhancement of the HDS activity over NiMo/ASA was reported recently when 4-methyl, 6-ethyl dibenzothiophene was used as a model compound (53).

Fluorination Effect

After fluorination, the total HDN conversion of MCHA increases slightly, while the conversion of CHE hydrogenation stays constant (Figs. 6a and 6b). This indicates that the hydrogenation of CHE occurs on a site different from the HDN of MCHA. A stronger promotion effect was observed with the ASA-supported catalysts than with their Al_2O_3-supported counterparts. The MCH and MCHE yields with and without fluorination are shown in Figs. 7a and 7b. The

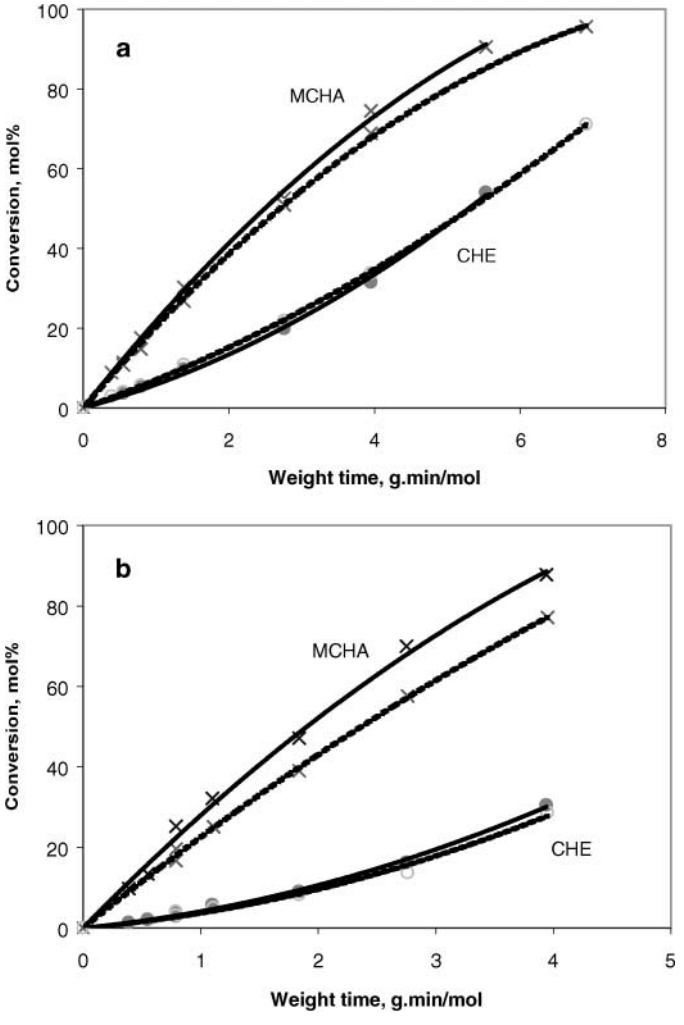

FIG. 6. Effect of fluorination on the hydrodenitrogenation of 14 kPa methylcyclohexylamine (MCHA) and the hydrogenation of 4 kPa cyclohexene (CHE) at 350°C over (a) NiMo/Al_2O_3 and (b) NiMo/ASA catalysts. (Solid lines) F-containing catalysts; (dashed lines) F-free catalysts.

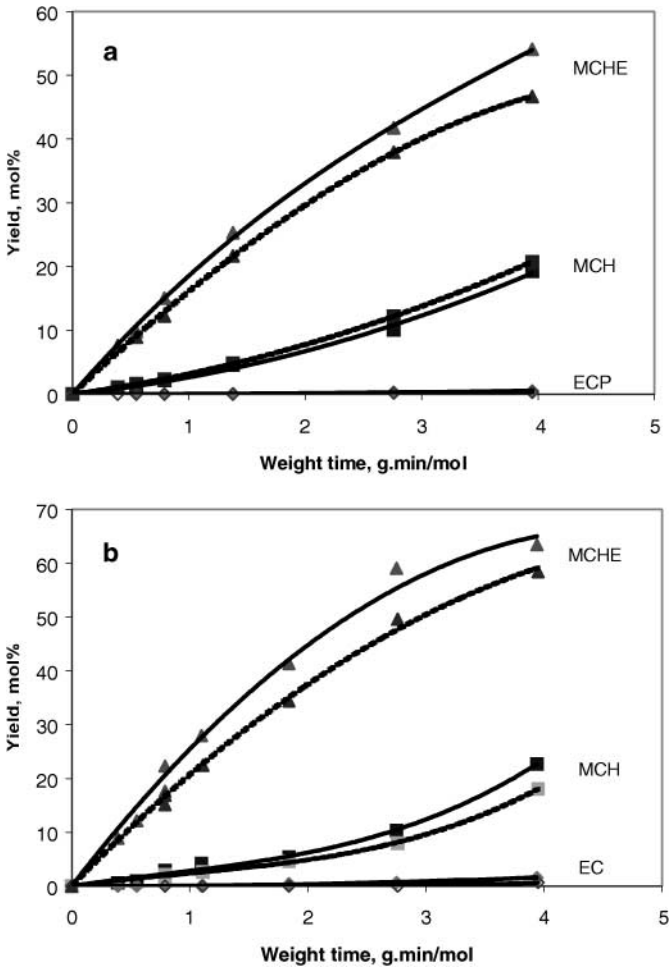

FIG. 7. Effect of fluorination on the yields of methylcyclohexene (MCHE) and methylcyclohexane (MCH) during the hydrodenitrogenation of 14 kPa methylcyclohexylamine (MCHA) at 350°C over (a) NiMo/Al_2O_3 and (b) NiMo/ASA catalysts. (Solid lines) F-containing catalysts; (dashed lines) F-free catalysts.

MCHE yield increased after fluorination while the MCH yield was not changed substantially in the HDN of MCHA over either the Al_2O_3- or the ASA-supported catalysts. This indicates that *in situ* fluorination mainly promotes the elimination path in the HDN of MCHA (Fig. 1).

Benitez *et al.* (22, 23) attributed the enhanced HDN activity of their *ex situ* fluorinated W/Al_2O_3 and NiW/Al_2O_3 catalysts to changes in the morphology of the WS_2 crystallites (higher stackings and larger sizes), a higher surface acidity, and also a better sulfidation of the W oxidic phase, which is promoted by the addition of fluoride to the alumina support, prior to the incorporation of the W precursor. Lewandowski and Sarbak studied the effect of fluorine on the hydrofining activity of a coal liquid over a NiMo/Al_2O_3 catalyst (28). They concluded that the enhanced HDN activity was caused by the higher acidity (mainly the Brønsted acidity) induced by fluoride addition to the alumina support, which promotes the C–N bond cleavage and also the resistance to coking. van Veen *et al.* (25) explained the role of fluorination by a transformation of the partly sulfided NiMoS phase to the more active, fully sulfided NiMoS phase. After breaking the Mo–O–Al linkages with the support, the NiMoS phase interacts with the support only via van der Waals forces. This may lead to increased stacking of the MoS_2 slabs and, thus, to a better accessibility of the sites for the adsorbent and to a higher HDN activity.

Even though in all cases ECP was present in a small amount only, an increase after fluorination could be observed. This is mainly caused by the increase in acidity by fluorination, which enhances the isomerization activity of the catalysts, as reported for the *ex situ* fluorination (27, 33, 54, 55).

When using fluorinated catalysts, fluorine leaching takes place but is not severe. For instance, a catalyst that originally contained 4.5 wt% F, retained 2.5 wt% F after 1 year onstream (8000 h) in a hydrotreating unit for diesel feed (private communication). At the same time, a corrosive test performed inside the reactor and in the downstream pipelines showed no influence on the materials of the reactor or pipelines. Furthermore, the possible effect of the leached fluorine on downstream catalysts like zeolites was negligible under severe conditions. For that reason, we did not measure the fluorine content after reaction. As judged from the above-mentioned industrial case, we believe that within our 3-week experiments there was no substantial loss of fluorine and, thus, no influence on the performance of the catalysts.

Kinetics of the HDN of MCHA

Kinetic modeling was based on the reaction scheme shown in Fig. 1. Since ECP was only detected at low concentrations at high MCHA conversion, it was not considered in the kinetic modeling. There are two different kinds of sites for the HDN of MCHA and hydrogenation of CHE. Assuming that the hydrogenation of MCHE takes place on the same sites as for CHE, which are different from the sites for the HDN of MCHA, we obtain the following Langmuir–Hinshelwood rate equations:

$$-\frac{dP_{\mathrm{MCHA}}}{d\tau} = \frac{(k_1+k_2)K_{\mathrm{MCHA}}P_{\mathrm{MCHA}}}{1+K_{\mathrm{MCHA}}P_{\mathrm{MCHA}}}, \quad [1]$$

$$\frac{dP_{\mathrm{MCHE}}}{d\tau} = \frac{k_1K_{\mathrm{MCHA}}P_{\mathrm{MCHA}}}{1+K_{\mathrm{MCHA}}P_{\mathrm{MCHA}}} - \frac{k_3K_{\mathrm{MCHE}}P_{\mathrm{MCHE}}}{1+K'_{\mathrm{MCHA}}P_{\mathrm{MCHA}}}, \quad [2]$$

$$\frac{dP_{\mathrm{MCH}}}{d\tau} = \frac{k_2K_{\mathrm{MCHA}}P_{\mathrm{MCHA}}}{1+K_{\mathrm{MCHA}}P_{\mathrm{MCHA}}} + \frac{k_3K_{\mathrm{MCHE}}P_{\mathrm{MCHE}}}{1+K'_{\mathrm{MCHA}}P_{\mathrm{MCHA}}}, \quad [3]$$

where k_1 and k_2 are the reaction rate constants for the elimination and the direct reaction pathways, respectively, and k_3 is the reaction rate constant for the hydrogenation of MCHE to MCH. K_i and K'_i are the adsorption equilibrium

TABLE 1

Fitted Parameters for the MCHA Reactions on $NiMo/Al_2O_3$

Catalyst		k_1 ($kPa \cdot mol \cdot g^{-1} \cdot min^{-1}$)	k_2 ($kPa \cdot mol \cdot g^{-1} \cdot min^{-1}$)	K_{MCHA} (kPa^{-1})	K'_{MCHA} (kPa^{-1})	MSC
$NiMo/Al_2O_3$	310°C	0.27 (0.01)	0.12 (0.01)	0.45 (0.05)	8.7 (3.8)	7.9
	330°C	0.94 (0.02)	0.22 (0.01)	0.24 (0.02)	1.2 (0.1)	7.3
	350°C	3.15 (0.08)	0.69 (0.05)	0.17 (0.01)	0.9 (0.1)	6.2
$FNiMo/Al_2O_3$	310°C	0.37 (0.01)	0.13 (0.01)	0.38 (0.04)	9.4 (2.2)	7.4
	330°C	1.24 (0.03)	0.27 (0.02)	0.23 (0.03)	2.4 (0.3)	7.0
	350°C	3.88 (0.12)	0.78 (0.05)	0.14 (0.01)	1.2 (0.2)	6.0

constants of compound i on the HDN sites and hydrogenation sites, respectively. Here, we assume that the adsorption constants for the elimination and the direct reaction are the same since there are no significant changes in the selectivity of MCHE when changing the initial partial pressure of MCHA. The values of the rate and adsorption equilibrium constants for the hydrogenation of MCHE (k_3 and K_{MCHE}) were taken from the results of CHE hydrogenation in our previous study (38). The adsorption equilibrium constant of NH_3 was assumed to be zero, because it is one magnitude smaller than that of MCHA (56, 57).

All the reactions were performed at a total pressure of 5.0 MPa and a partial pressure of hydrogen at the reactor inlet of 4.8 MPa. All the kinetic data were obtained after 20 h onstream, when the catalyst was stabilized at 350°C. No deactivation was observed during the experiments. Five initial partial pressures of MCHA were used at each temperature, and at each MCHA initial partial pressures more than five weight times were tested. The temperatures studied were 310, 330, and 350°C. Based on the thus-obtained data, kinetic modeling was performed with the SCIENTIST® program. The initial values for k_1 and k_2 were estimated from the initial conversions of MCHA at 36 kPa to MCHE and MCH, because at that high MCHA partial pressure the reactions can be approximated as being zero order and at low conversion the hydrogenation of MCHE can be neglected. Reaction rate constants for the two reaction pathways and adsorption equilibrium constants of MCHA on the HDN sites were obtained from the fitting of all data obtained at five initial partial pressures of MCHA, more than five weight times, and three temperatures, as indicated above. The results are presented in Tables 1 and 2. Numbers in parentheses indicate the standard deviations of the fitted parameters and MSC is the model selection criterion. The larger the value of MSC, the better the fit. The MSC is defined by the formula

$$\mathrm{MSC} = \ln\left(\frac{\sum_{i=1}^{n} w_i \left(Y_{obs_i} - \bar{Y}_{obs}\right)^2}{\sum_{i=1}^{n} w_i \left(Y_{obs_i} - Y_{cal_i}\right)^2}\right) - \frac{2p}{n},$$

where $\bar{Y}_{obs}$ is the weighted mean of the observed data Y_{obs_i}, Y_{cal_i} is the calculated data, p and n are the number of parameters and measured points in the model, respectively, and w_i is the weight factors applied to the points. All weight factors were put equal to one.

Illustrative fits are shown in Fig. 8. It is clear that MCHA has a strong inhibition on the hydrogenation of MCHE. The maximum of the MCHE intermediate is reached at different weight times at different MCHA partial pressures. When the conversion of MCHA is below 40%, the MCH yield varies linearly with weight time. Only when most of the MCHA has reacted away is an increase in the production rate of MCH observed.

Over the Al_2O_3-supported catalysts, at all three temperatures studied, the HDN reaction rate constants for the elimination increased by about 30% after fluorination, while

TABLE 2

Fitted Parameters for the MCHA Reactions on NiMo/ASA

Catalyst		k_1 ($kPa \cdot mol \cdot g^{-1} \cdot min^{-1}$)	k_2 ($kPa \cdot mol \cdot g^{-1} \cdot min^{-1}$)	K_{MCHA} (kPa^{-1})	K'_{MCHA} (kPa^{-1})	MSC
NiMo/ASA	310°C	0.33 (0.01)	0.08 (0.01)	0.60 (0.07)	8 (20)	8.3
	330°C	1.20 (0.01)	0.16 (0.03)	0.39 (0.04)	0.7 (0.3)	7.2
	350°C	3.85 (0.20)	0.39 (0.04)	0.26 (0.04)	0.1 (0.5)	6.2
FNiMo/ASA	310°C	0.49 (0.01)	0.10 (0.01)	0.35 (0.02)	12 (4)	8.8
	330°C	1.64 (0.01)	0.24 (0.02)	0.27 (0.01)	7 (2)	8.3
	350°C	5.52 (0.17)	0.50 (0.09)	0.16 (0.02)	0.7 (0.1)	5.3

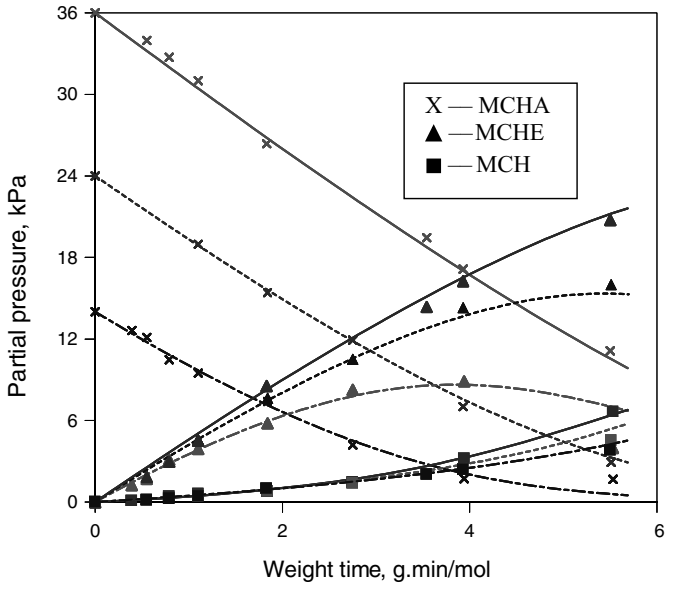

FIG. 8. An illustration of the fit for the hydrodenitrogenation of 14, 24, and 36 kPa methylcyclohexylamine over F–NiMo/ASA at 350°C. (Lines) Fitted curves; (points) experimental data.

those for the direct reaction increased less (Table 1). The adsorption equilibrium constants of MCHA remained almost unchanged by fluorination.

For the ASA-supported catalysts, the HDN rate constants for the elimination increased by more than 40% after fluorination, while those for the direct reaction increased less (Table 2). The ratio k_1/k_2 for the ASA-supported catalysts (with values between 4 and 11) was higher than that for the Al_2O_3-supported catalysts (between 2 and 5) at all temperatures. The adsorption equilibrium constants of MCHA on the HDN sites decreased after fluorination.

TABLE 3

Activation Energies and Preexponential Factors for the HDN of MCHA

		NiMo/ Al_2O_3	F–NiMo/ Al_2O_3	NiMo/ ASA	F–NiMo/ ASA
E (kJ · mol^{-1})	Path 1	186 (8)	177 (6)	186 (6)	183 (5)
	Path 2	132 (12)	135 (14)	118 (14)	122 (16)
A (kPa · mol · g^{-1} · min^{-1})	Path 1	1×10^{16}	1×10^{16}	1×10^{16}	1×10^{16}
	Path 2	3×10^{9}	9×10^{9}	3×10^{9}	6×10^{9}

Over all catalysts, the adsorption equilibrium constants of MCHA on the hydrogenation of MCHE are relative large compared with those on the HDN of MCHA itself, often with large errors. Because the majority of the kinetic data was obtained at MCHA conversions below 40%, it is clear the hydrogenation of MCHE to MCH plays only a minor role. As a consequence, uncertainties in k_3 and K'_{MCHA} have almost no influence on the parameters k_1, k_2, and K_{MCHA}, which are the main parameters of interest in our study.

With the Al_2O_3-supported as well as the ASA-supported catalysts, a weaker effect of fluorination was observed for the direct reaction than for the other reaction. This is caused by the different mechanisms of the two reactions. The direct reaction takes place via nucleophilic substitution of NH_2 by SH followed by C–S bond hydrogenolysis (46, 47). This is different from the reaction via the β-Hofmann elimination of NH_3 from MCHA. The former reaction is mainly determined by the partial pressure of H_2S in the reactor and not by the fluorination.

The activation energies of the HDN reaction paths were calculated from the Arrhenius plots of $\ln k$ versus $1/T$

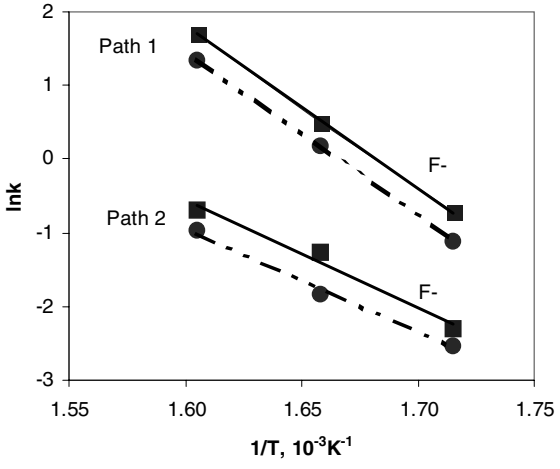

FIG. 9. Plot of $\ln k$ versus $1/T$ for the hydrodenitrogenation of methylcyclohexylamine over NiMo/ASA catalysts. (Solid lines) F-free catalysts; (dashed lines) F-containing catalysts.

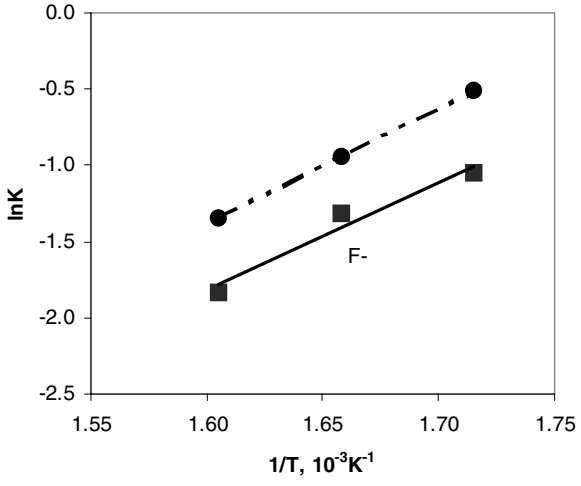

FIG. 10. Plot of $\ln K$ versus $1/T$ for the hydrodenitrogenation of methylcyclohexylamine over NiMo/ASA catalysts. (Solid lines) F-free catalysts; (dashed lines) F-containing catalysts.

TABLE 4

Heat of Adsorption

	NiMo/ Al_2O_3	F–NiMo/ Al_2O_3	NiMo/ ASA	F–NiMo/ ASA
$-\Delta H_{ads}$(kJ · mol^{-1})	77 (7)	75 (8)	63 (7)	59 (6)
K_0 (kPa^{-1})	6×10^{-8}	7×10^{-8}	1×10^{-6}	2×10^{-6}

(Fig. 9 and Table 3). Within the uncertainties of the measurements, the activation energies for paths 1 and 2 were independent of support and fluorination: about 180 kJ/mol for the elimination path and 130 kJ/mol for the direct path. This indicates that the catalytic sites on which MCHA react are the same for the Al_2O_3-supported as for the ASA-supported catalysts and are not influenced by the presence of fluorine. This confirms the general belief that fluorine is located on the support and not on the metal sulfide. The only effect of support and fluorine is to change the dispersion of the NiMo sulfide. Fluorination as well as changing the support from Al_2O_3 to ASA increases the number of sites active in the HDN of MCHA. Fluorine and the ASA support have about the same positive influence on the elimination path (cf. Tables 1 and 2), while NiMo on fluorinated ASA showed the largest k_1 values.

Like the activation energies, the heats of adsorption can be obtained from an Arrhenius plot of $\ln K$ versus $1/T$ (Fig. 10 and Table 4). The heat of adsorption of MCHA on the catalytic sites for HDN over all catalysts are about the same, 60 kJ/mol. This further confirms that the active sites for HDN of MCHA are not influenced by fluorination and the support, and only the number of active sites increases after fluorination and with ASA support.

CONCLUSIONS

The HDN of MCHA proceeds via two pathways, the elimination of NH_3 followed by the hydrogenation of MCHE to MCH and the direct reaction to MCH. Fitting of the kinetic data with Langmuir–Hinshelwood rate equations showed that the higher HDN activity over ASA-supported NiMo catalyst compared to its Al_2O_3-supported counterpart is due to the faster elimination of NH_3.

The promoting effect of fluorination is stronger for the elimination step than for the direct reaction. The promotion effect of fluorination arises from the increase in the number of sites active for the HDN of MCHA, while the intrinsic activity remains the same.

REFERENCES

1. Prins, R., *in* "Handbook of Heterogeneous Catalysis" (G. Ertl, H. Knözinger, and J. Weitkamp, Eds.), Vol. 4, p. 1908. VCH, Berlin, 1997.
2. Stanulonis, J. J., Tabacek, J. A., and Vogel, R. F., Gulf Research & Development Co., Pittsburgh, U.S. Patent 4,285,807 (1981).
3. Stanulonis, J. J., Tabacek, J. A., and Vogel, R. F., Gulf Research & Development Co., Pittsburgh, U.S. Patent 4,328,128 (1982).
4. Gulf Research & Development Co., Pittsburgh, PA, JP 56,037,049 (1981).
5. Shi, Y., Li, D., Liu, X., Nie, H., Gao, X., and Ying, Y., China Petrochemical Co., Beijing, PCT Int. Appl., WO 9,800,234 A1 (1998).
6. Shi, J., Nie, H., Zhang, Y., and Li, D., China Petrochemical Co., Beijing, CN 1,056,514 (1991).
7. Shi, Y., Li, D., Liu, X., Nie, H., Gao, X., and Ying, Y., China Petrochemical Co., Beijing, CN 1,169,336 (1998).
8. Wang, K., Liu, G., and Shi, Y., China Petrochemical Co., Beijing, CN 1,169,457 (1998).
9. Shi, J., Nie, H., Shi, Y., Shi, Y., Zhang, Y., and Li, D., China Petrochemical Co., Beijing, CN 1,169,458 (1998).
10. Xiong, Z., Liu, X., Zhang, Y., Nie, H., Ying, Y., He, Y., and Kang, X., China Petrochemical Co., Beijing, CN 1,221,020 (1999).
11. Song, X., Ding, L., and Lan, L., China Petrochemical Co., Fushun, CN 1,302,848 (2001).
12. Benazzi, E., and Mignard, S., Institut Français du Petrole, Eur. Patent 794,005 A1 (1997).
13. Kasztelan, S., George-Marchal, N., and Benazzi, E., Institut Français du Petrole, Eur. Patent 955,093 A1 (1999).
14. Kasztelan, S., Benazzi, E., and George-Marchal, Institut Français du Petrole, Eur. Patent 967,012 A1 (1999).
15. Bronner, C., Heinrich, G., Plain, C., and Carpot, L., Institut Français du Petrole, Eur. Patent 1,063,275 A1 (2000).
16. Kasztelan, S., Benazzi, E., and George-Marchal, Institut Français du Petrole, Eur. Patent 2,780,310 A1 (1999).
17. John, H., Becker, K., Birke, P., Berrouschot, H. D., Hattwig, M., Walkowski, L., Kuehn, H., Schuetter, H., and Franke, H., VEB Leuna-Werke "Walter Ulbricht," DD 227,888 A1 (1985).
18. Hoefpfner, E., Schuetter, H., Franke, H., Limmer, H., Hergeth, H., Doehler, E., Goltz, N., Bohlmann, D., and Matthey, R., VEB Petrochemisches Kombinat Schwedt, DD 262,443 A1 (1988).
19. Nebesh, E., Plundo, R. A., and McMahon, S. L., Engelhard Co., Eur. Patent 335,583 A1 (1989).
20. Loginova, A. N., Tomina, N. N., Sharikhina, M. A., Vlasov, V. G., Golubev, A. B., Levin, O. V., Vyazkov, V. A., Shafranskii, E. L., Oltyrev, A. G., Kitova, M. V., Popova, O. A., and Lukanov, A. A., Obshchestvo s Ogranichennoi Otvetstvennost'yu "Novokuibyshevskii Zavod Katalizatorov," RU 2,159,672 C1 (2000).
21. Ramirez, J., Cuevas, R., Lopez Agudo, A., Mendioroz, S., and Fierro, J. L. G., *Appl. Catal.* **57**, 223 (1990).
22. Benitez, A., Ramirez, J., Vazquez, A., Acosta, D., and Lopez Agudo, A., *Appl. Catal. A* **133**, 103 (1995).
23. Benitez, A., Ramirez, J., Fierro, J. L. G., and Lopez Agudo, A., *J. Catal.* **144**, 343 (1996).
24. Benitez, A., Ramirez, J., Cruz-Reyes, J., and Lopez Agudo, A., *J. Catal.* **172**, 137 (1997).
25. van Veen, J. A. R., Colijn, H. A., Hendriks, P. A. J. M., and van Welsenes, A. J., *Fuel Process. Technol.* **35**, 137 (1993).
26. Qu, L., Jian, M., Shi, Y., and Li, D., *Chinese J. Catal.* **19**, 608 (1998).
27. Fierro, J. L. G., Cuevas, R., Ramirez, J., and Lopez Agudo, A., *Bull. Soc. Chim. Belg.* **100**, 945 (1991).
28. Lewandowski, M., and Sarbak, Z., *Appl. Catal. A* **156**, 181 (1997).
29. Kwak, C., Kim, M. Y., Song, C. J., and Moon, S. H., *Stud. Surf. Sci. Catal.* **121**, 283 (1998).
30. Kwak, C., and Moon, S. H., *Korean J. Chem. Eng.* **16**, 608 (1999).
31. Matralis, H. K., Lycourghiotis, A., Grange, P., and Delmon, B., *Appl. Catal.* **38**, 273 (1988).
32. Matralis, H. K., Papadopoulou, Ch., and Lycourghiotis, A., *Appl. Catal.* **116**, 273 (1994).
33. Jiratova, K., and Kraus, M., *Appl. Catal.* **27**, 21 (1986).

34. Startsev, A. N., Klimov, O. V., Kalinin, A. V., and Mastikhin, V. M., *Kinet.Catal.* **35**, 601 (1994).
35. Ramirez, J., Cuevas, R., Gasque, L., Vrinat, M., and Breysse, M., *Appl. Catal*. **71**, 351 (1991).
36. Ladeur, P., Post, B., Fagot, M., and Saint, J. P., Shell International Research B. V., GB 2,024,642 (1979).
37. Bertolacini, R. J., Mosby, J. F., and Schwartz, J. G., Standard Oil Company, U.S. Patent 4,420,388 (1983).
38. Qu, L., and Prins, R., *J. Catal*. **207**, 286 (2002).
39. Rota, F., and Prins, R., *Top.Catal.* **11/12**, 327 (2000).
40. Rota, F., and Prins, R., *Stud. Surf. Sci. Catal.* **127**, 319 (1999).
41. Qu, L., and Prins, R., *Stud. Surf. Sci. Catal.* **133**, 139 (2001).
42. Portefaix, J.-L., Cattenot, M., Guerriche, M., Thivolle-Cazat, J., and Breysse, M., *Catal. Today* **10**, 473 (1991).
43. Nelson, N., and Levy, R. B., *J. Catal*. **58**, 485 (1979).
44. Vivier, L., Dominguez, V., Perot, G., and Kasztelan, S., *J. Mol. Catal.* **67**, 267 (1991).
45. Cattenot, M., Portefaix, J.-L., Breysse, M., Lacroix, M., and Perot, G., *J. Catal.* **173**, 366 (1998).
46. Rota, F., and Prins, R., *J. Mol. Catal. A* **162**, 359 (2000).
47. Rota, F., and Prins, R., *J. Catal.* **202**, 195 (2001).
48. Minderhoud, J. K., and van Veen, J. A. R., *Fuel Process. Technol.* **35**, 87 (1993).
49. Muralidhar, G., Massoth, F. E., and Shabtai, J., *J. Catal.* **85**, 44 (1984).
50. Massoth, F. E., Muralidhar, G., and Shabtai, J., *J. Catal.* **85**, 53 (1984).
51. Saiprasad Rao, K., and Murali Dhar, G., *J. Catal*. **115**, 277 (1989).
52. Rajagopal, S., Marini, H. J., Marzari, J. A., and Miranda, R., *J. Catal*. **147**, 417 (1994).
53. Robinson, W. R. A. M., van Veen, J. A. R., de Beer, V. H. J., and van Santen, R. A., *Fuel Process. Technol.* **61**, 89 (1999).
54. Boorman, P. M., Kydd, R. A., Sarbak, Z., and Somogyvari, A., *J. Catal*. **96**, 115 (1985).
55. Boorman, P. M., Kydd, R. A., Sarbak, Z., and Somogyvari, A., *J. Catal*. **106**, 544 (1987).
56. Sonnemans, J. F., van den Berg, G. H., and Mars, P., *J. Catal.* **31**, 220 (1973).
57. Satterfield, C. N., and Yang, S. H., *Ind. Eng. Chem. Process Des. Dev.* **23**, 11 (1984).